Mechanosensitivity of an Epithelial Na^+ Channel in Planar Lipid Bilayers: Release from Ca^{2+} Block

Iskander I. Ismailov, Bakhram K. Berdiev, Vadim Gh. Shlyonsky, and Dale J. Benos
Department of Physiology and Biophysics, The University of Alabama at Birmingham, Birmingham, Alabama 35294 USA

ABSTRACT A family of novel epithelial Na^+ channels (ENaCs) have recently been cloned from several different tissues. Three homologous subunits (α, β, γ-ENaCs) form the core conductive unit of Na^+-selective, amiloride-sensitive channels that are found in epithelia. We here report the results of a study assessing the regulation of α, β, γ-rENaC by Ca^{2+} in planar lipid bilayers. Buffering of the bilayer bathing solutions to $[Ca^{2+}] < 1$ nM increased single-channel open probability by fivefold. Further investigation of this phenomenon revealed that Ca^{2+} ions produced a voltage-dependent block, affecting open probability but not the unitary conductance of ENaC. Imposing a hydrostatic pressure gradient across bilayers containing α,β,γ-rENaC markedly reduced the sensitivity of these channels to inhibition by $[Ca^{2+}]$. Conversely, in the nominal absence of Ca^{2+}, the channels lost their sensitivity to mechanical stimulation. These results suggest that the previously observed mechanical activation of ENaCs reflects a release of the channels from block by Ca^{2+}.

INTRODUCTION

Transport of sodium across absorptive epithelia such as renal collecting tubules, frog skin, and toad urinary bladder plays an essential role in maintaining salt and water balance. The physiological importance of this process is reflected by the abundance of regulatory mechanisms that provide fine control over apical membrane-located amiloride-sensitive Na^+ channels, the rate-limiting step for net transepithelial Na^+ transport. One of these specific regulatory mechanisms involves small ions like H^+, Na^+, and Ca^{2+} that are present in the cytoplasm of these cells (Garty and Benos, 1988; Turnheim, 1991). The objective of the present study was to test the hypothesis that Ca^{2+} regulates ENaC, a recently cloned epithelial Na^+ channel. The channel comprises three homologous subunits (α, β, and γ), is highly selective for Li^+ and Na^+ over K^+, and is sensitive to inhibition by the diuretic drug amiloride (Canessa et al., 1993, 1994). We have found that 1) the activity of α, β, γ-rENaC can be modulated by *cis* and *trans* Ca^{2+}; 2) in the presence of a hydrostatic pressure gradient, both *cis* and *trans* Ca^{2+} inhibited α, β, γ-rENaC at significantly higher concentrations; 3) buffering of the *cis* and *trans* bilayer bathing solution to $[Ca^{2+}] < 1$ nM increased the initial level of α, β, γ-rENaC activity by fivefold and resulted in a loss of mechanosensitivity. These data suggest that the previously reported mechanosensitivity properties of these channels in bilayers (Awayda et al., 1995; Ismailov et al., 1996a) depend upon the presence of Ca^{2+}. We conclude that the activation of α, β, γ-rENaC after the imposition of a hydrostatic pressure gradient across a channel-containing bilayer may reflect a release of the channel from inhibition by Ca^{2+}.

Received for publication 15 August 1996 and in final form 11 December 1996.

Address reprint requests to Dr. Dale J. Benos, Department of Physiology and Biophysics, The University of Alabama at Birmingham, BHSB 706, UAB Station, Birmingham, AL 35294-0005. Tel.: 205-934-6220; Fax: 205-934-2377; E-mail: benos@phybio.bhs.uab.edu.

0006-3495/97/03/1182/11 $2.00

MATERIALS AND METHODS

Planar lipid bilayer experiments

Planar lipid bilayers were painted over a 200-μm aperture in the polystyrene chamber (the thickness of the partition at the aperture was 0.25 mm), using a phospholipid solution containing diphytanoylphosphatidylethanolamine, diphytanoylphosphatidylserine, and oxidized cholesterol in a 2:1:2 weight ratio (final lipid concentration = 25 mg/ml) in *n*-octane (Ismailov et al., 1996a). Lipids were purchased from Avanti Polar Lipids (Alabaster, AL). Bilayers were bathed with 100 mM NaCl containing 10 mM 3-(*N*-morpholino)propanesulfonic acid-Tris (MOPS-Tris) buffer (pH 7.4). All solutions were made using Milli-Q water and were filter-sterilized by passing through 0.22-μm filters (Sterivax-GS filters; Millipore Corporation, Bedford, MA). Submicromolar concentrations of free Ca^{2+} in the bilayer bathing solutions were determined by Fura-2 fluorescence measurements. Additions of Ca^{2+} to the desired level in the experiments with elevated $[Ca^{2+}]$ were made using calibrated $CaCl_2$ solution according to calculations by the Bound-And-Determined computer program (Brooks and Storey, 1992). The final free levels of $[Ca^{2+}]$ in the solutions in the micromolar range were verified by fluorometry with Fura-2. Current measurements were made with a high-gain amplifier circuit, as described elsewhere (Ismailov et al., 1995, 1996a). In all experiments the applied voltage refers to the *trans* chamber, which was connected to the current-to-voltage converter and therefore was held at virtual ground.

α-, β-, and γ-rENaC proteins were in vitro translated, using a micrococcal nuclease-treated rabbit reticulocyte cell lysate (Promega, Madison, WI) in the presence of canine microsomal membranes, and reconstituted into liposomes as described earlier (Awayda et al., 1995; Ismailov et al., 1996a). The reconstituted proteoliposomes were applied with a fire-polished glass rod to the *trans* side of a preformed bilayer with the membrane held at -40 mV. Under these experimental conditions, the channels were oriented with their amiloride-sensitive (extracellular) surface exposed to the *trans* compartment in over 90% of the incorporations. All of the analyses were performed for single active Na^+ channels, as was ascertained in each experiment by imposing a hydrostatic pressure gradient across the bilayer (Ismailov et al., 1996a). In all of the experiments performed to date (over 5000 reported here and elsewhere; see Ismailov et al., 1996a,b; Berdiev et al., 1996), α-, β-, γ-rENaC displayed three equally spaced subconductive states 13, 26, and 39 pS in magnitude. The imposition of a hydrostatic pressure gradient activated all of the channels in a

given membrane, including those initially "silent," and always revealed this three-core type of channel activity. Under no circumstances have any of these three conductance states been observed in isolation, i.e., independently of the other two. The effect of hydrostatic pressure was independent of the direction of the gradient, i.e., ΔP was equally effective when the level of the bilayer bathing solution was raised/lowered on either side of the channel-containing bilayer. Furthermore, activation of the channels residing in any given membrane was fully reversible. Removal of 1 ml of the bathing solution from one of the compartments (18.8 mm in diameter and 18 mm in depth; the aperture was located 11.5 mm from the top edge of the cup) is equivalent to a hydrostatic pressure difference of 0.26 mm Hg.

Acquisition and analysis of single-channel recordings were performed using pCLAMP software and hardware (Axon Instruments, Foster City, CA), as described previously (Ismailov et al., 1996a). Briefly, single-channel records were stored unfiltered on Beta VCR tape, using a Vetter model 20 digital data recorder (Vetter Instruments), played back low-pass-filtered at 300-Hz frequency through an 8-pole Bessel filter (902 LPF; Frequency Devices, Haverhill, MA), and sampled at 1 kHz using a Digidata 1200 interface (Axon Instruments). Single-channel analysis was performed on records 3–15 min in duration. Single-channel current was normalized for each experiment under any given specified condition from at least 3 min of continuous recording, using the equation

$$I_{norm} = \bar{I}/(N \cdot i), \quad (1)$$

where N is total number of channels (always equal to 1 in these experiments), $\bar{I}$ is the mean current over the period of observation, and I is the maximum state unitary current determined from all-points current amplitude histograms produced by pCLAMP. The mean current ($\bar{I}$) over the period of observation was calculated using the events list generated by pCLAMP software and the equation

$$\bar{I} = \frac{\sum_m^M i_m \cdot t_m}{\sum t_m}, \quad (2)$$

where i_m is an event current (all levels, including the zero current level); t_m is an event dwell time, and M is the total number of events. An averaged I_{norm} was computed from N independent experiments. Event analysis was performed on records of at least 10-min duration, with event detection thresholds set at 50% of the amplitude of transition between levels and 3 ms for event duration. The bin widths in the event dwell-time histograms were 5 ms.

The kinetic treatment of the data obtained at different $[Ca^{2+}]$ was performed using the equation of Michaelis-Menten, rewritten as follows:

$$I_{norm} = I_{norm}^{max} \cdot \left(1 - \frac{[Ca^{2+}]}{K_i^{Ca} + [Ca^{2+}]}\right), \quad (3)$$

where I_{norm} is the normalized single-channel current at a given concentration of Ca^{2+}, $[Ca^{2+}]$; I_{norm}^{max} is a maximum normalized single-channel current in the nominal absence of Ca^{2+}; and K_i^{Ca} is the equilibrium inhibitory constant of Ca^{2+}. As a first approximation, we assume that the concentration of Ca^{2+} at the surface of the membrane equals that in the bathing solution, and that the activity coefficient for Ca^{2+} is 1.

An analysis of the data obtained at different holding potentials was performed following the formulation of Woodhull (1973), assuming that the binding site for Ca^{2+} lies within the electric field:

$$K_d(V) = K_d(0)\exp(\delta z FV/RT), \quad (4)$$

where $K_d(V)$ is the Ca^{2+} inhibitory dissociation constant at a given holding potential; $K_d(0)$ is the Ca^{2+} inhibitory dissociation constant at zero holding potential; δ is the fraction of the electric distance between the binding site for the inhibitor and the channel surface; z is the valence of the inhibitor (i.e., +2 for Ca^{2+}); T is the absolute temperature; and F, V, and R have their usual meanings.

RESULTS

Effects of $[Ca^{2+}]$ on α, β, γ-rENaC

α, β, γ-rENaC in bilayers displayed three subconductive states of 13, 26, and 39 pS, with a characteristic gating pattern (Fig. 1, *top trace*) that could be described with a triple-barrel model (Ismailov et al., 1996a). This current record was obtained under control conditions when the bilayer containing a single α, β, γ-rENaC was bathed with standard 100 mM NaCl solutions containing 11 ± 4 μM Ca^{2+}, as measured by Fura-2. Buffering the solutions bathing both sides of the bilayer with 10 mM EGTA increased the normalized current of ENaC (I_{norm}) from 0.12 ± 0.02 to

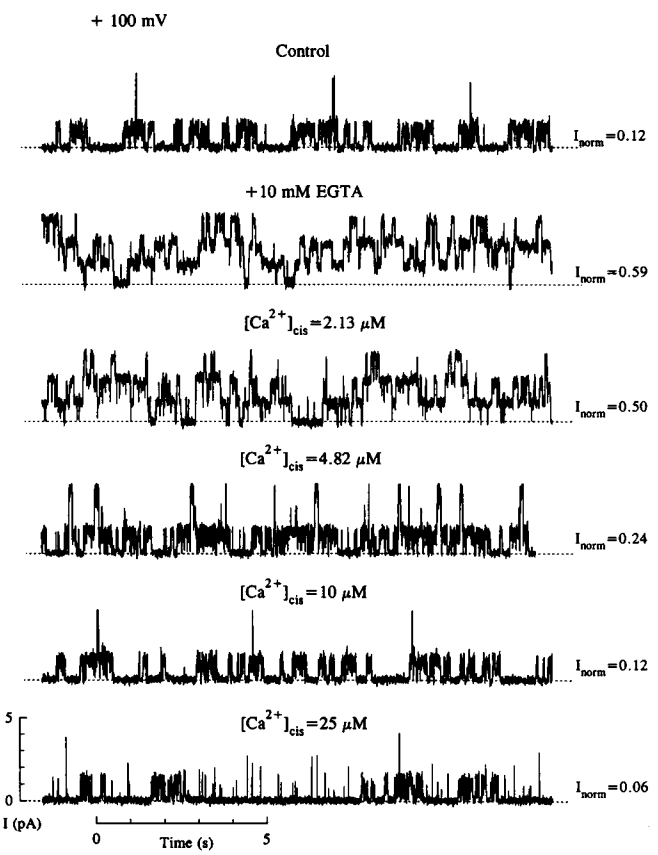

FIGURE 1 Effect of $[Ca^{2+}]$ on α, β, γ-rENaC reconstituted into planar lipid bilayers. Traces are representative of at least eight separate experiments with single-channel current recordings at different $[Ca^{2+}]_{cis}$. Bilayers were bathed with 100 mM NaCl containing 10 mM MOPS-Tris buffer (pH 7.4). Holding potential was +100 mV referred to the *trans* chamber, which was held at virtual ground through the current-to-voltage converter. The analog signal was filtered at 300 Hz with an 8-pole Bessel filter before acquisition, at 1 ms per point, using pCLAMP software and hardware. For illustration purposes, records were digitally filtered at 100 Hz by using pCLAMP software. Numbers next to traces represent normalized current through single α, β, γ-rENaC (I_{norm}) for each experimental condition, which was calculated for at least 3 min of continuous recording using Eq. 1. The final free Ca^{2+} concentration for each experimental condition is indicated above each trace. Free $[Ca^{2+}]$ at concentrations less than 10 μM was measured with Fura-2. Additions needed to achieve the desired level of $[Ca^{2+}]_{free}$ were calculated by using the Bound-and-Determined computer program (Brooks and Storey, 1992).

0.61 ± 0.05 (Fig. 1, *second trace*; $N = 13$). Elevating the concentration of Ca^{2+} in either compartment of the bilayer chamber resulted in a dose-dependent decrease in I_{norm}, but not in the unitary conductance of the channels. The records obtained in one of these experiments in which increasing additions of Ca^{2+} were made to the *cis* compartment (i.e., to the presumptive "intracellular" face of ENaC) are shown in Fig. 1. The additions of Ca^{2+} to the *trans* compartment produced similar effects on channel gating, although with a different dose dependence. Moreover, the effectiveness of both *trans* and *cis* Ca^{2+} as a blocker of ENaC was dependent upon membrane voltage. The resultant *trans* and *cis* Ca^{2+} dose-response curves obtained at four different holding potentials are shown in Fig. 2, *A* and *B*, respectively. Fitting the experimental data to the Michaelis-Menten equation (Eq. 3) permitted the calculation of $[Ca^{2+}]$ required for half-maximum inhibition of the channels (K_i^{Ca}). These K_i values were different, depending on whether Ca^{2+} was added to the *cis* or to the *trans* bathing solution. As indicated above, these values were also dependent on the voltage at which the channel-containing bilayer was held. For instance, $K_{i,trans}^{Ca}$ was 92.3 ± 11.3 μM ($N = 7$) at +100 mV and 3.8 ± 0.6 μM ($N = 8$) at −100 mV; $K_{i,cis}^{Ca}$ was 4.6 ± 0.9 μM ($N = 6$) at + 100 mV and 48.7 ± 7.3 μM ($N = 6$) at −100 mV. Fig. 2 *C* depicts semilogarithmic plots of *cis* and *trans* K_i^{Ca} as a function of membrane voltage. The lines through the data points were computed from Eq. 4, using a best-fit approach and varying δ. An implicit assumption of this analysis is that the binding sites are located within the electric field. It is evident that there was an inverse voltage dependence between *cis* and *trans* inhibition of ENaC by Ca^{2+}, suggesting a minimum of two binding sites within the electric field. The placement of these two sites computed by this fit is at 14.7 ± 1.5% and 19.8 ± 1.3% of the electrical distance from the *cis* and *trans* surfaces of the channel, respectively. Therefore, these results are consistent with the hypothesis that Ca^{2+} directly modulates ENaC in a manner similar to that of amiloride-sensitive channels in native cells (Ismailov et al., 1995; Silver et al., 1993).

We next attempted to find possible explanations that could account for the observation that under nominally Ca^{2+}-free conditions α, β, γ-rENaC fluctuates randomly between four equally spaced conductance levels (including the zero-current level). The previously proposed model (Ismailov et al., 1996a) describing the kinetic behavior of α, β, γ-rENaC was as follows:

$$\underset{(0\ pS)}{\text{Level 0}} \underset{k_1}{\overset{k}{\rightleftharpoons}} \underset{(13\ pS)}{\text{Level 1}} \underset{l_1}{\overset{l}{\rightleftharpoons}} \underset{(26\ pS)}{\text{Level 2}} \underset{m_1}{\overset{m}{\rightleftharpoons}} \underset{(39\ pS)}{\text{Level 3}}, \quad (5)$$

where Level 0 represents the closed state, and Levels 1 through 3 the 13-, 26-, and 39-pS open states, respectively. One of the assumptions of this model was that the channel comprised three identical, separate conduction units. If this assumption is correct, some predictions could be made with regard to channel kinetics. First, for a channel that consists of three identical conduction units, each with one open and

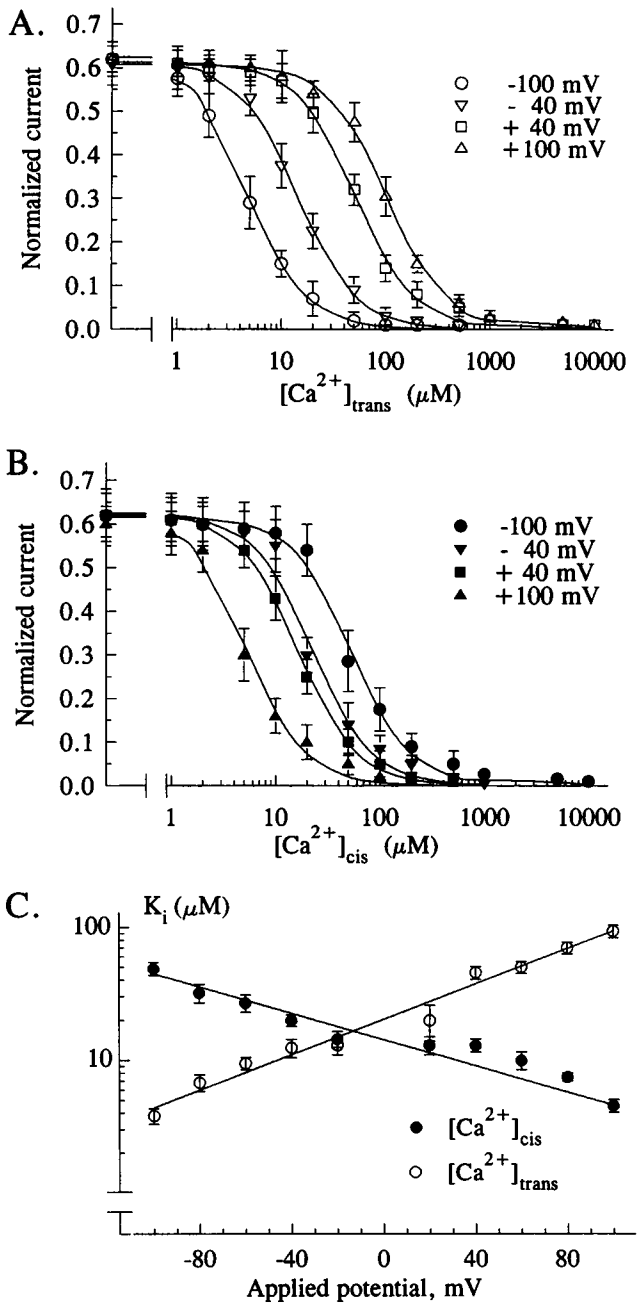

FIGURE 2 Voltage-dependent block of α, β, γ-rENaC by Ca^{2+}. Data points and error bars in $[Ca^{2+}]_{trans}$ (*A*) and $[Ca^{2+}]_{cis}$ (*B*) dose-response curves represent mean ± SD I_{norm} for each holding potential, computed from at least six independent experiments. The lines through the data points represent fits of the data obtained at different free $[Ca^{2+}]$ (performed using Eq. 3). (*C*) Voltage dependences of $K_{i,trans}^{Ca}$ and $K_{i,cis}^{Ca}$. Data points and error bars represent mean ±SD K_i^{Ca} for *cis* and *trans* Ca^{2+}, computed from at least six independent experiments using Eq. 3. The lines through the data points were computed from Eq. 4, using a best-fit approach

one closed state, the overall kinetics scheme can be rewritten as

$$\text{Level 0} \underset{k_{off}}{\overset{3k_{on}}{\rightleftharpoons}} \text{Level 1} \underset{2k_{off}}{\overset{2k_{on}}{\rightleftharpoons}} \text{Level 2} \underset{3k_{off}}{\overset{k_{on}}{\rightleftharpoons}} \text{Level 3}, \quad (6)$$

where k_{on} and k_{off} are the rate constants for the opening and closure, respectively, of an individual unit.

The probability that the channel is in any of these four states must be equal to unity:

$$P_o^o + P_o' + P_o'' + P_o''' = 1, \tag{7}$$

where P_o^o, P_o', P_o'', and P_o''' are the probabilities for the channel resident in levels 0 through 3, respectively.

These probabilities can be calculated as ratios of the fraction of time spent by α, β, γ-rENaC in a given state (t_o, t_1, t_2, and t_3 for levels 0 through 3, respectively) to the total time of observation (T):

$$\begin{Bmatrix} P_o^o = t_o/T \\ P_o' = t_1/T \\ P_o'' = t_2/T \\ P_o''' = t_3/T \end{Bmatrix}, \tag{8}$$

and can be extracted from single-channel recordings by all-points histogramming (Fig. 4 *A*).

For a triple-barrel channel, these probabilities should conform to a binomial distribution:

$$\begin{Bmatrix} P_o^o = (1-p)^3 \\ P_o' = 3p(1-p)^2 \\ P_o'' = 3p^2(1-p) \\ P_o''' = p^3 \end{Bmatrix}, \tag{9}$$

where p is the open probability of an individual unit, and P_o^o, P_o', P_o'', and P_o''' are the probabilities for the channel resident in levels 0 through 3, respectively.

Substituting the P_o for the values determined by Eq. 8 suggests that each conduction unit has an open probability equal to 0.5. This means that the rate constants for transition of each conduction unit from its closed state into its open state or back, are equal:

$$k_{on} = k_{off}. \tag{10}$$

Moreover, the relationship between the directly assessable time constants for channel residence in each conductance level and the rate constants underlying openings and closures of individual units according to Eq. 5 due to intrinsic gating can be predicted as follows:

$$\begin{Bmatrix} 1/\tau_0 = 3k_{on} \\ 1/\tau_1 = 2k_{on} + k_{off} \\ 1/\tau_2 = k_{on} + 2k_{off} \\ 1/\tau_3 = 3k_{off} \end{Bmatrix}. \tag{11}$$

Equations 10 and 11 have a unique solution, namely, that $\tau_0 = \tau_1 = \tau_2 = \tau_3$.

Indeed, in the nominal absence of free Ca^{2+}, the dwell time histograms for all four conductance levels were fit well by a single exponential formulation:

$$y = a \exp(-x/\tau), \tag{12}$$

with the time constants of 55, 54, 57, and 53 ms for the conductance levels 0 through 3, respectively (Fig. 3 *A*). These data support our initial assumption that a single α, β, γ-rENaC is composed of three identical conduction units.

However, in earlier experiments, only a few transitions to Level 2 were observed, unless the channel was exposed to micromolar concentrations of the sulfhydryl reducing agent dithiotreitol or to 1.5 M salt (Ismailov et al., 1996a). These agents presumably affect association of protein molecules. Thus we hypothesized that the 26-pS transition (Level 1 → Level 3) was composed of two concertedly linked conduction units of 13 pS each, and that the opening to Level 1 was produced by a single 13-pS conduction unit. Thus we simplified the scheme to contain two predominant transitions: one of 13 pS and another of 26 pS. When both of them are open, the maximum conductance state of the channel is 39 pS:

$$\underset{(0\ pS)}{\text{Level 0}} \underset{k_1}{\overset{k}{\rightleftharpoons}} \underset{(13\ pS)}{\text{Level 1}} \underset{m_1}{\overset{m}{\rightleftharpoons}} \underset{(39\ pS)}{\text{Level 3}}. \tag{13}$$

One possibility is that buffering of all free Ca^{2+} in the bilayer bathing solution with EGTA could affect the association of conduction units, thus producing independence in their gating, similar to what was observed with DTT-treated α, β, γ-rENaC. On the other hand, the voltage dependence of the *cis* and *trans* Ca^{2+} effects on α, β, γ-rENaC provides

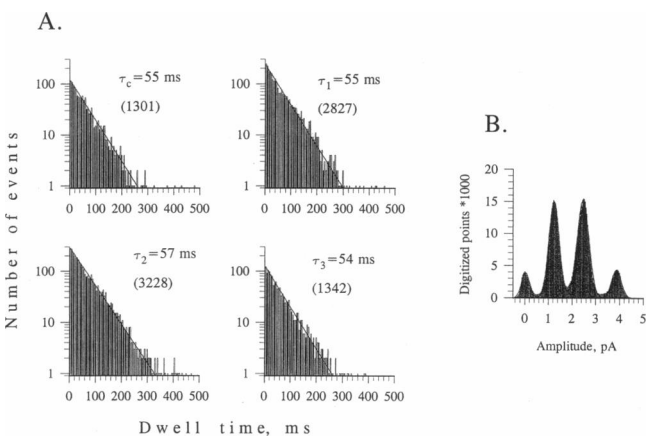

FIGURE 3 Kinetic properties of α, β, γ-rENaC reconstituted into planar lipid bilayer. Dwell-time histograms for levels 0 through 3 (*A*) were constructed following events analysis performed using pCLAMP software (Axon Instruments) on a single-channel recording of 10-min duration. Bilayers were bathed with 100 mM NaCl containing 10 mM MOPS-Tris buffer (pH 7.4) and 10 mM EGTA. The holding potential was +100 mV, referred to the *trans* chamber. The analog signal was filtered at 300 Hz with an 8-pole Bessel filter before acquisition at 1 ms per point using pCLAMP software and hardware. Event detection thresholds were 50% in amplitude of transition between levels and 3 ms for event duration. The bin width in event dwell time histograms was 5 ms. The histograms for all conductance levels were fit well by a single exponential formulation (Eq. 12). Time constants for the fits are shown in each plot for the conductance levels 0 through 3, respectively. Numbers in parentheses represent the number of events used for construction of the histogram for each level. An all-points amplitude histogram (*B*) was constructed by pCLAMP on the channel record analyzed in *A*. Bin width was 0.033 pA.

evidence for Ca^{2+} block of the channel within its conduction pathway. Release of the channel from this block may be considered an alternative mechanism underlying the observed change-of-gating phenomena. Both hypotheses are testable in terms of single-channel kinetics.

Congruent with the above postulate of independence for each conduction unit, the kinetics of α, β, γ-rENaC can be analyzed in terms of the block of each conduction unit, conforming to the basic model of open-channel blockade:

$$\text{Open} \underset{k_U}{\overset{k_B}{\rightleftharpoons}} \text{Blocked}, \tag{14}$$

similar to that described for inwardly rectified K^+ channel (Matsuda, 1988; Matsuda and Cruz, 1988). The terms k_B and k_U represent blocking and unblocking rate constants, respectively, and can be extracted from the single-channel recordings from directly assessable blocked (τ_B) and unblocked (τ_U) time constants:

$$\tau_B = k_U^{-1} \tag{15}$$

$$\tau_U = (a + k_B[\text{Blocker}])^{-1}. \tag{16}$$

In these terms, the overall kinetics scheme of a triple-barrel channel blockade can be rewritten as

$$\text{Open} \underset{k'_U}{\overset{k'_B}{\rightleftharpoons}} \text{Blocked}_1 \underset{k''_U}{\overset{k''_B}{\rightleftharpoons}} \text{Blocked}_2 \underset{k'''_U}{\overset{k'''_B}{\rightleftharpoons}} \text{Blocked}, \tag{17}$$

where Blocked_2, Blocked_1, and Open are the 13-, 26-, and 39-pS conductance levels, respectively.

The rate constants for the channel transitions between four conductance states due to Ca^{2+} block can be calculated as follows:

$$\begin{Bmatrix} 1/\tau_0 = k'_B \\ 1/\tau_1 = k''_B + k'_U \\ 1/\tau_2 = k'''_B + k''_U \\ 1/\tau_3 = k'''_U \end{Bmatrix}. \tag{18}$$

The hypothesis of complete independence for each conduction unit of α, β, γ-rENaC also presumes that each unit can be independently blocked by Ca^{2+}. Therefore, the rate constants k'_B, k'_U; k''_B, k''_U; k'''_B, k'''_U for the transitions between these states due to Ca^{2+} block should also conform to a binomial distribution:

$$\begin{Bmatrix} k'_B = 3k_B \\ k''_B = 2k_B \\ k'''_B = 1k_B \end{Bmatrix} \tag{19}$$

and

$$\begin{Bmatrix} k'_U = 1k_U \\ k''_U = 2k_U \\ k'''_U = 3k_U \end{Bmatrix}, \tag{20}$$

where k_B and k_U are the blocking and unblocking rates of each unit (Eq. 14).

Fig. 4 shows the results of testing this hypothesis. Dwell-time histograms were constructed for all four conductance levels of α, β, γ-rENaC at 2.13 μM *cis* $[Ca^{2+}]$. It is evident from the graphs that the histograms for levels 0 through 2 do not conform to a single-exponential distribution (Eq. 12), but can be fit using a double-exponential equation:

$$y = a_1 \exp(-x/\tau_1) + a_2 \exp(-x/\tau_2). \tag{21}$$

On the other hand, the histogram for level 3 follows a single-exponential distribution (Eq. 12). The nature of a double-exponential fit can be understood from the fact that the long time constants for channel residence in all four conductance levels were essentially identical and equal to the time constants in the nominal absence of Ca^{2+}. These results are suggestive that these time constants relate to the intrinsic gating of α, β, γ-rENaC, rather than to block of the channel by Ca^{2+}. Moreover, the short time constants apparent in all of the histograms for Levels 1 and 2 (but not for Level 0), and the time constants for the fully opened state of

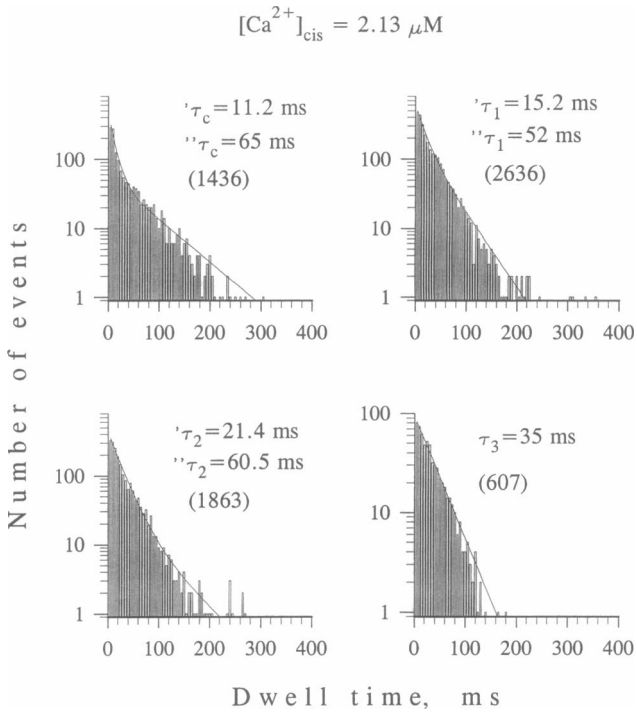

FIGURE 4 Effect of Ca^{2+} on kinetic properties of α, β, γ-rENaC. Dwell-time histograms were constructed following events analysis performed using pCLAMP software (Axon Instruments) on a single-channel recording of 10-min duration. Bilayers were bathed with 100 mM NaCl containing 10 mM MOPS-Tris buffer (pH 7.4), 10 mM EGTA, and 2.13 μM free Ca^{2+}. The holding potential was +100 mV. Data treatment, analysis, and presentation of the results was the same as indicated for Fig. 3 *A*. The histograms for levels 0 through 2 were fit using a double-exponential equation (Eq. 21). The histogram for level 3 was fit by a single-exponential distribution (Eq. 12). Time constants for the fits are shown in each plot. Numbers in parentheses represent the number of events used for the construction of the histogram for each level.

TABLE 1 Kinetic analysis of Ca^{2+} block of α, β, γ-rENaC reconstituted into planar lipid bilayer

$[Ca^{2+}]_{cis}$ (μM)	Voltage (mV)	τ_0 (ms)	τ_1 (ms)	τ_2 (ms)	τ_3 (ms)	k_B (M^{-1} s^{-1})	k_U (s^{-1})
2.13	+100	11.2	15.2 (14.5)	21.4 (20.5)	35.0	**9.5**	**29.7**
	+80	8.7	12.1 (11.6)	18.1 (18.0)	39.0	**8.5**	**38.7**
	+60	7.5	10.1 (10.4)	17.5 (16.9)	44.2	**7.5**	**44.4**
4.82	+100	11.6	19.8 (14.1)	15.5 (17.9)	24.5	**13.6**	**28.7**
	+80	8.5	22.5 (11.1)	27.7 (16.2)	29.4	**11.3**	**39.2**
	+60	7.4	26.6 (10.0)	31.1 (15.4)	33.2	**10.0**	**45.0**
10.0	+100	12.2	17.5 (13.9)	−(16.3)*	19.5	**17.1**	**27.3**
	+80	8.4	21.1 (10.7)	−(14.7)*	23.7	**14.1**	**39.7**
	+60	6.9	26.7 (9.3)	−(14.2)*	30.2	**11.0**	**48.3**

Time constants for levels 0 through 3 (τ_0 to τ_3, respectively) were calculated from exponential fits (Eqs. 12 and 21) of the dwell-time histograms constructed after event analysis performed using pCLAMP software (Axon Instruments) on single-channel recording of 10-min duration at each $[Ca^{2+}]_{free}$. Recording conditions, data treatment, and analysis were as indicated for Fig. 3 *A*. Blocking (k_B) and unblocking (k_U) constants were calculated from τ_3 and τ_0, respectively. Numbers in parentheses represent predictions of binomial theory (Eqs. 18–20) for three independent conduction units.
*Low occurrence of event observation precluded statistically significant histogram analysis.

the channel demonstrated their dependence on $[Ca^{2+}]$ and applied voltage (Table 1). Taking into account all of these considerations, we concluded that the constant for the short exponent of the closed time can serve as a measure of the channel Ca^{2+} blocked time, whereas the constant for the fully open state reflects the channel Ca^{2+} unblocked time. Furthermore, theoretically predicted time constants calculated using Eqs. 18–20 (Table 1, in parentheses) were in good agreement with the time constants measured experimentally. The highest correlation was observed for levels 0 and 3, and in the presence of less than 5 μM Ca^{2+}. Moreover, at higher $[Ca^{2+}]$, the channel essentially does not reveal its residence in level 2. We consider these results as indicative of two mechanisms that can account for effects of Ca^{2+} on the gating of α, β, γ-rENaC: direct block of the channel at low concentrations and effects on the association of the channel conduction units.

$[Ca^{2+}]$ is required for mechanical activation of α, β, γ-rENaC

We next tested the hypothesis that the sensitivity of ENaC to inhibition by *cis* or *trans* Ca^{2+} was different under an imposed hydrostatic pressure gradient (ΔP) because other biophysical channel parameters (e.g., amiloride inhibition, cation permeability) could be altered by mechanical stimulation (Ismailov et al., 1996a). To test this hypothesis, we performed similar experiments (those described above) only in the presence of a ΔP. Initially, upon mechanical stimulation, α, β, γ-rENaC resides with equal probability of being in one of its three conductance states (Fig. 5, *second trace*), similar to what has previously been reported (Ismailov et al., 1996a). This effect of ΔP was symmetrical and completely reversible (not shown). Buffering of the bilayer bathing solutions with 10 mM EGTA in the presence of ΔP did not affect P_o of ENaC (Fig. 5, *third trace*). However, similar to what was found in the absence of a

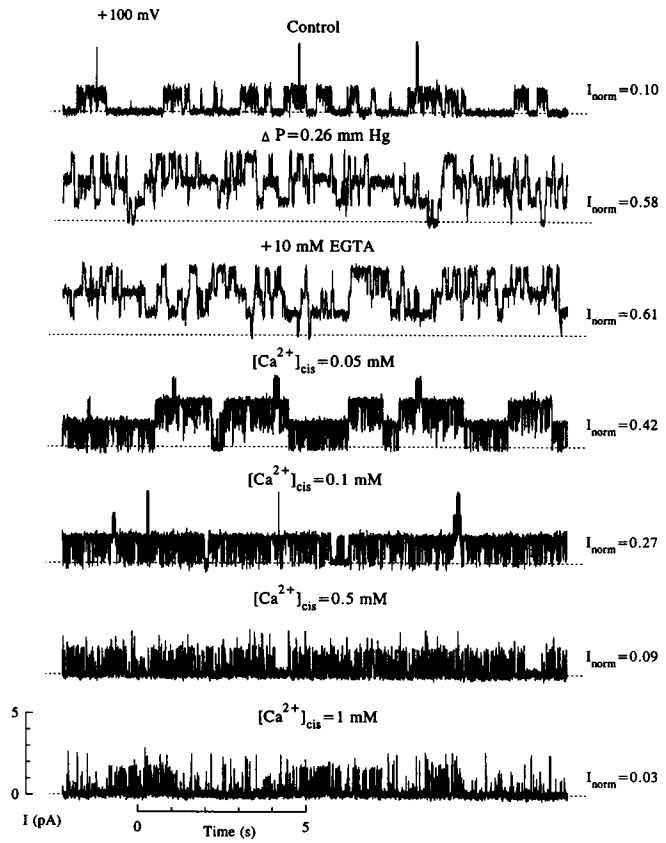

FIGURE 5 Effect of $[Ca^{2+}]$ on α, β, γ-rENaC reconstituted into planar lipid bilayers in the presence of a hydrostatic pressure gradient. Traces are representative of at least seven separate experiments at different $[Ca^{2+}]_{cis}$. Recording conditions, additions of Ca^{2+}, and treatment of the records were the same as indicated for Fig. 1. Quantitation of ΔP was based on the calculation that removal of 1 ml of the bathing solution from one of the compartments (18.8 mm in diameter and 18 mm in depth, the aperture was placed 11.5 mm from the top edge) is equivalent to a hydrostatic pressure difference of 0.26 mm Hg.

hydrostatic pressure gradient (cf., Fig. 1), either *cis* or *trans* Ca^{2+} successfully inhibited the channel, but only at very high concentrations ($\gg$10 μM). As before, this inhibition affected channel gating, but not its unitary conductance. A representative set of single α, β, γ-rENaC current records generated in the presence of ΔP when $[Ca^{2+}]$ was increased in the *cis* compartment is shown in Fig. 5. Summary dose-response curves constructed from these experiments performed with *trans* or *cis* Ca^{2+} in the presence of a ΔP are shown in Fig. 6. As in the absence of ΔP, K_i^{Ca} depended upon what side of the bilayer Ca^{2+} was added, and on the holding potential. Thus $K_{i,trans}^{Ca}$ was 1.9 $\pm$ 0.3 mM (N = 6) at +100 mV and 85.3 $\pm$ 11.2 μM (N = 9) at −100 mV. $K_{i,cis}^{Ca}$ was 91.2 $\pm$ 21.1 μM (N = 8) at +100 mV, and 1.1 $\pm$ 0.2 mM (N = 7) at −100 mV (the direction of ΔP was *trans* to *cis*). Semilogarithmic plots of *cis* and *trans* K_i^{Ca} as a function of membrane voltage at different directions of ΔP (Fig. 7) reveal that the placement of Ca^{2+}-binding sites within the conduction pathway of the mechanically stimulated ENaC depended on the direction of ΔP. The electrical distances from the presumptive cytoplasmic and extracellular surface of the channel were 20.1 $\pm$ 0.9% and 16.1 $\pm$ 0.7%, respectively, when ΔP was direct from *cis* to *trans*. These values became 15.3 $\pm$ 0.4% and 19.8 $\pm$ 0.7% when the direction of ΔP was reversed. However, these distances were identical to those calculated in the absence of ΔP.

The analysis of channel blockade kinetics was performed according to the model described above (Eqs. 14 through 20). Fig. 8 depicts the dwell-time histogram constructed for α, β, γ-rENaC in the presence of *trans*-to-*cis* hydrostatic pressure gradient and in the presence of 50 μM $[Ca^{2+}]_{cis}$. All histograms followed a single exponential formulation (Eq. 12). Similar to those observed in the absence of ΔP (although at lower $[Ca^{2+}]$), the time constants obtained at different $[Ca^{2+}]$ depended on the holding potential (Table 2). Moreover, these constants for the times spent by α, β,

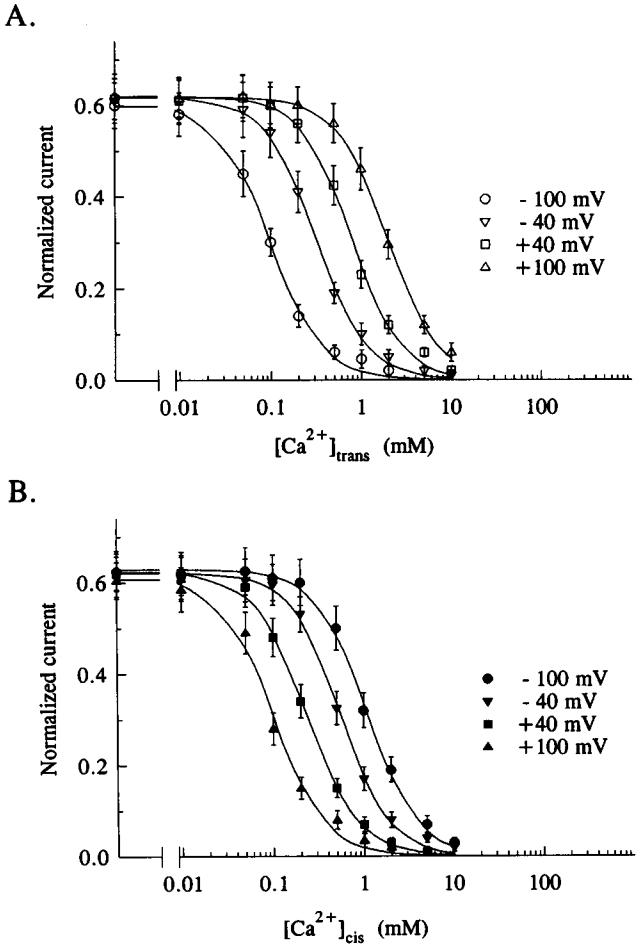

FIGURE 6 Voltage-dependent block of α, β, γ-rENaC by Ca^{2+} in the presence of a hydrostatic pressure gradient. Effect of holding potential on $[Ca^{2+}]_{trans}$ (*A*) and $[Ca^{2+}]_{cis}$ (*B*) dose-response curves. Data points and error bars in the graphs represent mean $\pm$ SD I_{norm} for each holding potential computed from at least six independent experiments. The lines through the data points represent fits of the data using Eq. 3. A hydrostatic pressure gradient of 0.26 mm Hg was imposed by a removal of 1 ml of the bathing solution from the *cis* compartment.

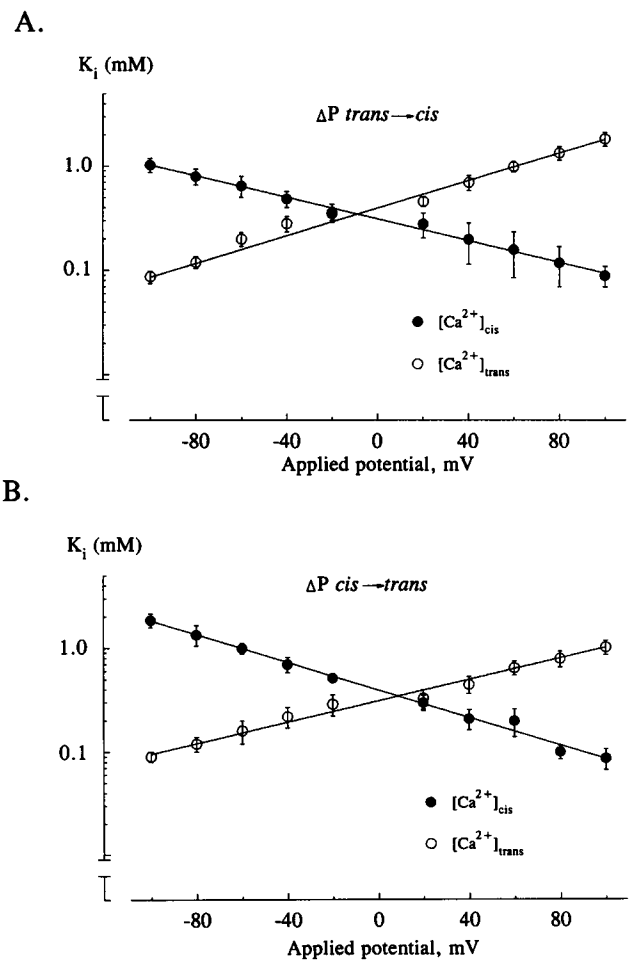

FIGURE 7 Effect of a hydrostatic pressure gradient on voltage dependences of $K_{i,trans}^{Ca}$ and $K_{i,cis}^{Ca}$. Data points and error bars represent mean $\pm$ SD K_i^{Ca} for *cis* and *trans* Ca^{2+} computed using Eq. 3, from at least six independent experiments under each experimental condition. The lines through the data points were computed from Eq. 4, using a best-fit approach.

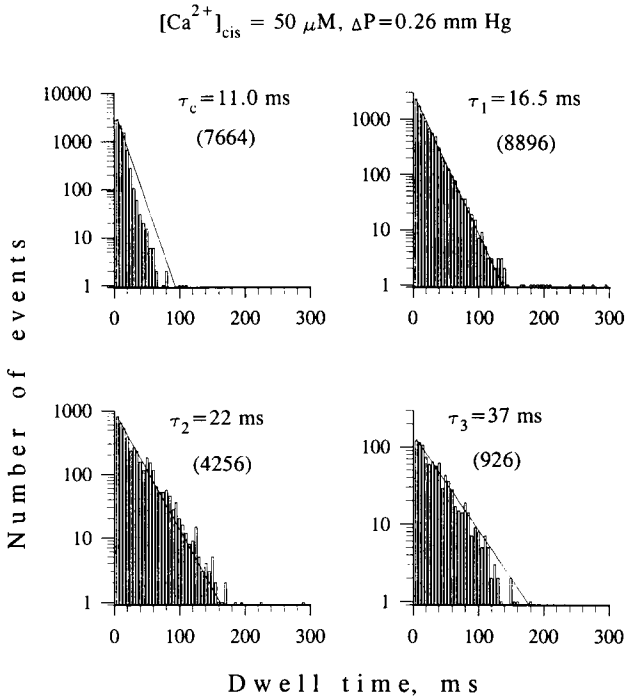

FIGURE 8 Effect of Ca^{2+} on kinetic properties of α, β, γ-rENaC in the presence of a hydrostatic pressure gradient. Dwell-time histograms for levels 0 through 3 were constructed following events analysis performed using pCLAMP software (Axon Instruments) on a 10-min-long single-channel recording. The bathing solution contained 100 mM NaCl, 10 mM MOPS-Tris buffer (pH 7.4), 10 mM EGTA, and 50 μM free Ca^{2+}. Recording conditions were as indicated for Fig. 5. Data treatment, analysis, and presentation of the results was the same as indicated for Fig. 3 *A*. Time constants for the single exponential fits (Eq. 12) are shown in each plot. Numbers in parentheses represent the number of events used for construction of the histogram for each level.

γ-rENaC in any of four states (including the zero-current level) conformed to a binomial distribution (the values predicted by calculation using Eqs. 18–20 are shown in parentheses). Thus, even in the presence of ΔP, the results support our hypothesis of multimeric organization of α, β, γ-rENaC.

A comparison of current records of the mechanically stimulated channel and resting ENaC in the presence of EGTA (cf. Figs. 1 and 5) revealed a striking similarity in the gating characteristics of the channel. Moreover, these records were similar to those that resulted from mechanical stimulation of the channel in the presence of Ca^{2+} (Fig. 5). Furthermore, the addition of EGTA did not affect the activity of the mechanically stimulated channel in any way. These observations prompted us to reverse the order of our manipulations, i.e., imposing a ΔP across an α, β, γ-rENaC-containing bilayer subsequent to the addition of 10 mM EGTA (Fig. 9). As before, the ENaC could be activated either by an increase in ΔP or by a reduction in free $[Ca^{2+}]$, displaying an increase in normalized current from 0.11 ± 0.03 to 0.62 ± 0.04 (N = 9) and from 0.12 ± 0.02 to 0.63 ± 0.04 (N = 8), respectively. The effect of either maneuver was completely reversible. After EGTA addition, the subsequent imposition of a ΔP did not have any effect whatsoever on the activity of the channel.

The ratios of $K_{i,\,trans}^{Ca}$ to $K_{i,\,cis}^{Ca}$ of the mechanically stimulated and the resting ENaC are 20.1 and 20.8, respectively. Therefore, mechanical stimulation appears to alter both binding sites for Ca^{2+} uniformly. This consideration predicts that by increasing $[Ca^{2+}]$ to a calculated level of 220 μM in both compartments of the bilayer chamber in the presence of ΔP, the "normal" gating of the channel should be restored. The experimental data obtained by testing this prediction are shown in Fig 10. Indeed, increasing $[Ca^{2+}]$ to 220 μM in both compartments of the bilayer chamber after mechanical activation restored the gating of the channel to what it was under control conditions, i.e., in the presence of $[Ca^{2+}]$ = 11 μM, with ΔP = 0.

DISCUSSION

Direct interaction of *cis* and *trans* Ca^{2+} with cloned epithelial Na^+ channels

The role of Ca^{2+} in the regulation of epithelial Na^+ channels has been extensively discussed in the literature. Curran

TABLE 2 Effect of a hydrostatic pressure gradient on kinetics of Ca^{2+} block of α,β,γ-rENaC reconstituted into planar lipid bilayer

$[Ca^{2+}]_{cis}$ (μM)	Voltage (mV)	τ_0 (ms)	τ_1 (ms)	τ_2 (ms)	τ_3 (ms)	k_B (M^{-1} s^{-1})	k_U (s^{-1})
10	+100	12.1	15.6 (16.0)	21.4 (23.5)	44.2	**7.5**	**27.5**
	+80	8.8	12.4 (12.2)	20.1 (19.5)	49.4	**6.7**	**37.9**
	+60	6.8	10.0 (9.6)	15.7 (16.2)	52.6	**6.3**	**49.0**
50	+100	11.0	16.5 (14.4)	22.0 (20.7)	37.0	**9.0**	**30.3**
	+80	9.1	12.3 (12.4)	19.9 (19.2)	43.2	**7.7**	**36.6**
	+60	7.0	10.3 (9.8)	15.6 (16.3)	48.8	**6.8**	**47.6**
100	+100	11.4	17.6 (15.1)	19.7 (19.4)	27.0	**12.3**	**29.2**
	+80	8.7	13.5 (12.7)	18.7 (18.1)	31.1	**10.7**	**38.3**
	+60	7.1	10.7 (9.7)	16.9 (15.3)	36.3	**9.2**	**46.9**

Time constants for levels 0 through 3 (τ_0 to τ_3, respectively) were calculated from exponential fits (Eqs. 12 and 21) of the dwell-time histograms constructed after event analysis performed using pCLAMP software (Axon Instruments) on single-channel recording of 10-min duration at each $[Ca^{2+}]_{free}$. Recording conditions, data treatment, and analysis were as indicated in legends for Figs. 5 and 8. Blocking (k_B) and unblocking (k_U) constants were calculated from τ_3 and τ_0, respectively. Numbers in parentheses represent theoretically predicted dwell times according to binomial theory (Eqs. 18–20) for three independent conduction units.

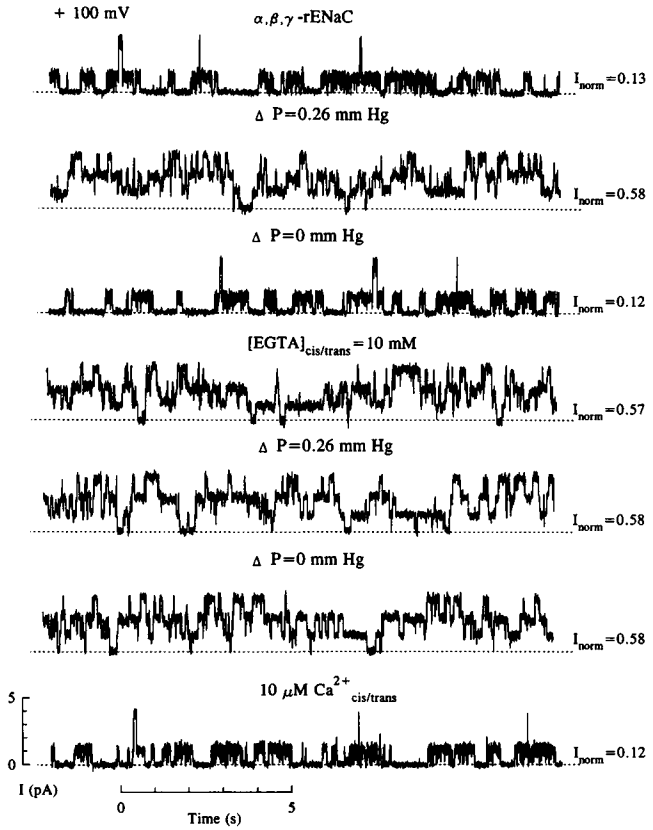

FIGURE 9 Effect of $[Ca^{2+}]$ on mechanosensitivity properties of α, β, γ-rENaC in planar lipid bilayers. Traces are representative of at least seven independent experiments with the same sequence of manipulations. Bilayer bathing solutions and all other recording conditions were as indicated in the legend to Fig. 1. A hydrostatic pressure gradient across a bilayer containing single α, β, γ-rENaC was imposed/discontinued by the removal/addition of 1 ml of bathing solution from/to the *trans* compartment. Additions of 10 mM EGTA (*fourth trace*) and 10 μM Ca^{2+} (*bottom trace*) were made to both the *cis* and *trans* compartments. Numbers next to the traces represent normalized current through single α, β, γ-rENaC (I_{norm}) for each experimental condition, which was calculated for at least 3 min of continuous recording using Eq. 1.

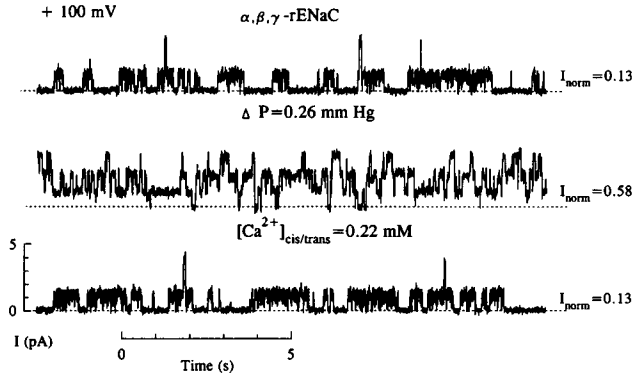

FIGURE 10 Effect of high Ca^{2+} on the activity of α, β, γ-rENaC in the presence of ΔP. Traces are representative of at least five separate experiments. The addition of 0.22 mM Ca^{2+} (*bottom trace*) was made to both the *cis* and *trans* compartments.

and colleagues (Curran and Gill, 1962; Curran et al., 1963) observed a decrease in the sodium permeability of frog skin after elevation of extracellular $[Ca^{2+}]$. Later studies of "feedback inhibition" of amiloride-sensitive Na^+ channels in the toad bladder (Grinstein and Erlij, 1978; Taylor and Windhager, 1979; Garty and Asher, 1985, 1986; Garty et al., 1987) attributed down-regulation of these channels exclusively to a rise in intracellular $[Ca^{2+}]$. More recent patch-clamp measurements of amiloride-sensitive Na^+ channels in rat cortical collecting tubule (Palmer and Frindt, 1987) and A6 cells (Ling and Eaton, 1989) have shown that Ca^{2+} does not appear to interact with these channels directly, but rather through other intracellular mediators. However, the interpretation of the data obtained in all of the aforementioned studies was complicated by unavoidable and uncontrolled variables resulting from the inherent complexity of the intact cell or native membrane. Therefore, the use of the planar lipid bilayer model system and the cell-free in vitro translated ENaC protein provides the opportunity to examine the effects of Ca^{2+} on these channels directly, independent of changes in cellular pH, membrane voltage, or variable number of channels present in a patch. The results of the present study suggest the direct interaction of both *cis* and *trans* Ca^{2+} with a cloned epithelial Na^+ channel, although this conclusion does not rule out the possibility that other components of the intracellular regulatory machinery can also participate in this interaction, as was the case for the immunopurified renal Na^+ channel (Ismailov et al., 1995).

Another finding of the present study was the determination of the exact range of concentrations that either *cis* or *trans* Ca^{2+} blocked ENaC. The K_i for "intracellular" Ca^{2+} at a physiologically relevant membrane potential of −60 mV was 27 ± 4 μM, which is two or three orders of magnitude higher than the normal range of intracellular $[Ca^{2+}]$. The K_i for "extracellular" Ca^{2+} at this voltage, on the other hand, was 10 ± 1 μM, two orders of magnitude lower than typical values of extracellular $[Ca^{2+}]$ (~1 mM). Therefore, these results suggest that under physiological conditions ENaC should always be closed, unless other regulatory pathways supersede the inhibitory influence of extracellular Ca^{2+}. The hypothesis that an imposed hydrostatic pressure gradient would alter the blocking affinities of Ca^{2+} was based on the previous observations of mechanically induced changes in amiloride inhibition (Ismailov et al., 1996a). Under mechanically activated conditions, the K_i for "intracellular" Ca^{2+} at −60 mV became 620 ± 130 μM, over 20-fold higher than that observed in the absence of a ΔP. The K_i for "extracellular" Ca^{2+} became 220 ± 27 μM, which was still significantly lower than prevailing extracellular $[Ca^{2+}]$ found in mammalian extracellular fluids. The position of the two presumptive binding sites for Ca^{2+} within the electric field of the channel was identical under resting or mechanically activated conditions. This finding confirms the specificity of the observed inhibition of ENaC by Ca^{2+}, in spite of the range of inhibiting Ca^{2+} concentrations. On the other hand, the K_i values reported in the

literature for extracellular Ca^{2+} inhibition of amiloride-sensitive Na^+ current in frog skin (Palmer, 1985) were in the range of 0.1 M. The reason for this disparity in inhibitory constants remains obscure, although it is obvious that under mechanically activated conditions, α, β, γ-rENaC is less sensitive to inhibition by Ca^{2+}. Furthermore, as mentioned above, other regulatory inputs such as protein kinase C phosphorylation may influence Ca^{2+}-dependent inhibition of ENaC in a manner similar to that reported for the immunopurified renal Na^+ channel (Ismailov et al., 1995).

[Ca^{2+}] control of the mechanosensitivity of cloned epithelial Na^+ channels

Mechanical properties of ENaCs are of special interest, because of the high homology of these proteins with MEC family degenerins found in *Caenorhabditus elegans* (Canessa et al., 1993; Lingueglia et al., 1995; Corey and Garcia-Anoveros, 1996). Although the α-subunit of ENaC was shown to form functional chimera channels with MEC-4 proteins (Waldman et al., 1995), the most well-documented evidence for mechanosensitivity of ENaCs was found in planar lipid bilayer experiments (Awayda et al., 1995; Ismailov et al., 1996a). On the other hand, there was no consistent effect of mechanical perturbation on amiloride-sensitive Na channels in rat cortical collecting tubules, known as prototypical epithelial Na channel (Palmer and Frindt, 1996). The statistical outcome of these experiments was as follows: 15 experiments revealed no effect of pressure on the channels in excised patches, whereas in six experiments the channel activity was reversibly increased. Lipid bilayer membranes, first described by Mueller et al. (1963), are very fluid structures at mechanical equilibrium (Fettiplace et al., 1971; Tien, 1974; Evans and Skalak, 1979). These structures consist of the planar bilayer itself, surrounded by a thick torus formed by the parent lipid solution, called the Plateau-Gibbs border (Tien, 1968). Therefore, a ΔP should apply relatively little physical strain on the incorporated protein molecule(s). However, in the experiments reported herein, α, β, γ-rENaC demonstrates high sensitivity to "stretch." The question arises, what are the physical events that underlie the mechanical activation of $\alpha\beta\gamma$-rENaC?

Several considerations should be mentioned with regard to transduction of ΔP on α, β, γ-rENaC. The channel is probably not responding to the pressure gradient per se, but to some microscopic mechanical distortion of the bilayer. If the membrane is formed of a volume V of lipid solution across the aperture, which is a right cylinder of radius R and height T such that $T \approx R$, one can assume that the volume of the bimolecular film is negligible compared with the volume of the Plateau-Gibbs border. When ΔP is applied, the Plateau-Gibbs border "supplies" the bulk of the lipid for the bilayer to expand, bow, and form a new curved surface at a new mechanical equilibrium. However, it is unrealistic to suppose that the Plateau-Gibbs border contains enough lipid solution for the bilayer to expand to the size that can equilibrate a 1-ml (or even a 0.5-ml) difference in the volume between compartments. In any case, the curvature of the membrane changes, while the membrane remains under pressure. The tension of the membrane at this new equilibrium will vary inversely with the curvature according to the law of Laplace. These considerations suggest that mechanosensitive channels may be responding to membrane curvature (Martinac et al., 1990; Markin and Martinac, 1991).

The observations that Ca^{2+} removal by the addition of EGTA did not activate ENaC beyond that observed with ΔP, and that under mechanically activated conditions α,β,γ-rENaC was less sensitive to inhibition by Ca^{2+}, led us to hypothesize that mechanical activation involves Ca^{2+}. The inhibition by Ca^{2+} has been reported for stretch-activated channels found in A6 cells (Kawahara and Matsuzaki, 1993; Marunaka et al., 1994), in *Xenopus* oocytes (Tagletti and Toselli, 1988; Yang and Sachs, 1989), and in frog lens epithelium (Rae et al., 1992). In our experiments under standard recording conditions, α,β,γ-rENaC was inhibited by $\sim$10 μM Ca^{2+} present in both bathing solutions. Imposition of ΔP lowers ENaC's sensitivity to Ca^{2+}. Therefore, upon mechanical activation, the channel may be activated because of a "release" from the Ca^{2+} inhibition that occurs at prevailing [Ca^{2+}]. This hypothesis was supported by the gating pattern of ENaC observed under resting and mechanically activated conditions in the presence of EGTA, and under stretched conditions in the absence of EGTA. Indeed, buffering all of the free Ca^{2+} in the bathing solution before the imposition of a ΔP across a bilayer containing a single α,β,γ-rENaC eliminated mechanoactivation of the channel. Moreover, increasing free [Ca^{2+}] to the level calculated from the ratios of $K_{i,\,trans}^{Ca}$ to $K_{i,\,cis}^{Ca}$ under resting and mechanically activated conditions (i.e., 220 μM *cis* and *trans* under mechanically activated conditions) restored the "normal" gating of the channel.

In conclusion, these data suggest that the activity of α, β, γ-rENaC can be modulated by "cytoplasmic" and "extracellular" Ca^{2+}. The previously observed activation of hese channels after the imposition of a hydrostatic pressure gradient across a channel-containing bilayer may reflect a release of Ca^{2+} block.

The authors gratefully acknowledge Dr. Bernard Rossier (University of Lausanne, Lausanne, Switzerland) for the kind gift of α-, β-, and γ-rENaC cDNAs and Drs. James K. Bubien (UAB), James A. Schafer (UAB), Sidney A. Simon (Duke University), H. Ti Tien (Michigan State University), and Ravshan Z. Sabirov (National Institute of Physiological Sciences, Japan) and the Editorial Board of the *Biophysical Journal* for helpful discussions and constructive criticisms of the manuscript.

This work was supported by National Institutes of Health grant DK 37206. Vadim Gh. Shlyonsky was on leave from the Institute of Physiology and Biophysics of the Uzbek Academy of Sciences, Tashkent, Uzbekistan.

REFERENCES

Awayda, M. S., I. I. Ismailov, B. K. Berdiev, and D. J. Benos. 1995. A cloned renal epithelial Na^+ channel protein displays stretch activation in planar lipid bilayers. *Am. J. Physiol.* 268:C1450–C1459.

Berdiev, B. K., A. G. Prat, H. F. Cantiello, D. A. Ausiello, C. M. Fuller, B. Jovov, D. J. Benos, and I. I. Ismailov. 1996. Regulation of epithelial sodium channels by short actin filaments. *J. Biol. Chem.* 271: 17704–17710.

Brooks, S. P., and K. B. Storey. 1992. Bound and determined: a computer program for making buffers of defined ion concentrations. *Anal. Biochem.* 201:119–126.

Canessa, C. M., J.-D. Horisberger, and B. C. Rossier. 1993. Epithelial sodium channel related to proteins involved in neurodegeneration. *Nature.* 361:467–470.

Canessa, C. M., L. Schild, G. Buell, B. Thoreus, I. Gantschl, J.-D. Horisberger, and B. C. Rossier. 1994. Amiloride-sensitive epithelial Na^+ channel is made of three homologous subunits. *Nature.* 367:463–467.

Corey, D. P., and J. Garcia-Anoveros. 1996. Mechanosensation and the DEG/ENaC ion channels. *Science.* 273:323–361.

Curran, P. F., and J. R. Gill. 1962. The effect of calcium on sodium transport by frog skin. *J. Gen. Physiol.* 45:625–645.

Curran, P. F., F. C. Herrera, and W. J. Flanigan. 1963. The effect of calcium and antidiuretic hormone on Na^+ transport across frog skin. II. Sites and mechanisms of action. *J. Gen. Physiol.* 46:1011–1027.

Evans, E. A., and R. Skalak. 1979. Mechanics and thermodynamics of biomembranes: part 1. *Crit. Rev. Bioeng.* 3:181–330.

Fettiplace, R., D. M. Andrews, and D. A. Haydon. 1971. The thickness fluctuations, composition and structure of some lipid bilayers and natural membranes. *J. Membr. Biol.* 5:277–296.

Garty, H., and C. Asher. 1985. Ca^{2+}-dependent, temperature-sensitive regulation of Na^+ channels in tight epithelia. *J. Biol. Chem.* 260: 8330–8335.

Garty, H., and C. Asher. 1986. Ca^{2+}-induced down-regulation of Na^+ channels in toad bladder epithelium. *J. Biol. Chem.* 261:7400–7406.

Garty, H., C. Asher, and O. Yeger. 1987. Direct inhibition of epithelial Na^+ channels by a pH-dependent interaction with calcium, and by other divalent ions. *J. Membr. Biol.* 96:151–162.

Garty, H., and D. J. Benos. 1988. Characteristics and regulatory mechanisms of the amiloride-blockable Na^+ channel. *Physiol. Rev.* 65: 309–373.

Grinstein, S., and D. Erlij. 1978. Intracellular calcium and the regulation of sodium transport in the frog skin. *Proc. R. Soc. Lond. B Biol. Sci.* 202:353–360.

Ismailov, I. I., M. S. Awayda, B. K. Berdiev, J. K. Bubien, J. E. Lucas, C. M. Fuller, and D. J. Benos. 1996a. Triple-barrel organization of ENaC, a cloned epithelial Na^+ channel. *J. Biol. Chem.* 271:807–816.

Ismailov, I. I., M. S. Awayda, B. Jovov, B. K. Berdiev, C. M. Fuller, J. R. Dedman, M. A. Kaetzel, and D. J. Benos. 1996b. Regulation of epithelial sodium channels by the cystic fibrosis transmembrane conductance regulator. *J. Biol. Chem.* 271:4725–4732.

Ismailov, I. I., B. K. Berdiev, and D. J. Benos. 1995. Regulation by Na^+ and Ca^{2+} of renal epithelial Na^+ channels reconstituted into planar lipid bilayers. *J. Gen. Physiol.* 106:445–466.

Kawahara, K., and K. Matsuzaki. 1993. A stretch-activated cation channel in the apical membrane of A6 cells. *Jpn. J. Physiol.* 43:817–832.

Ling, B. N., and D. C. Eaton. 1989. Effects of luminal Na^+ on single Na^+ channels in A6 cells, a regulatory role for protein kinase C. *Am. J. Physiol.* 256:F1094–F1103.

Lingueglia, E., N. Voilley, R. Waldman, M. Lazdunski, and P. Barbry. 1995. Expression cloning of an amiloride-sensitive Na^+ channel. A new channel type with homologies to *Caenorhabditis elegans* degenerins. *FEBS Lett.* 318:95–99.

Markin, V. S., and B. Martinac. 1991. Mechanosensitive ion channels as reporters of bilayer expansion. A theoretical model. *Biophys. J.* 60: 1120–1127.

Martinac, B., J. Adler, and C. Kung. 1990. Mechanosensitive ion channels of *E. coli* activated by amphipaths. *Nature.* 348:261–263.

Marunaka, Y., H. Tohda, N. Hagivara, and T. Nakahari. 1994. Antidiuretic hormone-responding nonselective cation channel in distal nephron epithelium (A6). *Am. J. Physiol* 35:C1513–C1522.

Matsuda, H. 1988. Open-state substructure of inwardly rectified potassium channels revealed by magnesium block in guinea-pig heart cells. *J. Physiol. (Lond.).* 397:237–258.

Matsuda, H., and J. D. S. Cruz. 1988. Voltage-dependent block by internal Ca^{2+} ions of inwardly rectified potassium K^+ in guinea-pig ventricular cells. *J. Physiol. (Lond.).* 470:295–311.

Mueller, P., D. O. Rudin, H. T. Tien, and W. C. Wescott. 1963. Methods fot the formation of single bimolecular lipid membranes in aqueous solution. *J. Phys. Chem.* 67:534.

Palmer, L. G. 1985. Modulation of apical Na^+ permeability of the toad urinary bladder by intracellular Na, Ca, and H. *J. Membr. Biol* 83:57–69.

Palmer, L. G., and G. Frindt. 1987. Effects of cell Ca^{2+} and pH on Na^+ channels from rat cortical collecting tubule. *Am. J. Physiol.* 253: F333–F339.

Palmer, L. G., and G. Frindt. 1996. Gating of Na^+ channels in the rat cortical collecting tubule: effects of voltage and membrane stretch. *J. Gen. Physiol.* 107:35–45.

Rae, J. L., R. T. Mathias, K. Cooper, and G. Baldo. 1992. Divalent cation effects on lens conductance and stretch-activated cation channels. *Exp. Eye. Res.* 55:135–144.

Silver, R. B., G. Frindt, E. E. Windhager, and L. G. Palmer. 1993. Feedback regulation of Na^+ channels in rat CCT. I. Effects of inhibition of Na pump. *Am. J. Physiol.* 264:F557–F564.

Tagletti, V., and M. Toselli. 1988. A study of stretch-activated channels in the membrane of frog oocytes: interactions with Ca^{2+} ions. *J. Physiol (Lond.).* 407:311–328.

Taylor, A., and E. E. Windhager. 1979. Possible role of cytosolic calcium and Na-Ca exchange in regulation of transepithelial sodium transport. *Am. J. Physiol.* 236:F505–F512.

Tien, H. T. 1968. Black lipid membranes at bifaces. Formation characteristics, optical and some thermodynamical properties. *J. Gen. Physiol.* 52:S125–S143.

Tien, H. T. 1974. Bilayer Lipid Membranes. Theory and Practice. Marcel Dekker, New York.

Turnheim, K. 1991. Intrinsic regulation of apical sodium entry in epithelia. *Physiol. Rev.* 71:429–449.

Waldman, R., G. Champigny, and M. Lazdunski. 1995. Functional degenerin-containing chimeras identify residues essential for amiloride-sensitive Na^+ channel function. *J. Biol. Chem.* 270:11735–11737.

Woodhull, A. M. 1973. Ionic blockade of sodium channel in nerve. *J. Gen. Physiol.* 61:687–708.

Yang, X. C., and F. Sachs. 1989. Block of stretch-activated ion channels in *Xenopus* oocytes by gadolinium and calcium ions. *Science.* 243: 1068–1071.